Available online at www.sciencedirect.com
SciVerse ScienceDirect
Procedia CIRP 7 (2013) 545 – 550

www.elsevier.com/locate/procedia

Forty Sixth CIRP Conference on Manufacturing Systems 2013

Contact-less and Programming-less Human-Robot Collaboration

Bernard Schmidt[a,]*, Lihui Wang[a,b]

[a] *Virtual Systems Research Centre, University of Skövde , PO Box 408, 541 28 Skövde, Sweden*
[b] *Department of Production Engineering, Royal Institute of Technology , Brinellvägen 68, 100 44 Stockholm, Sweden*
* Corresponding author. Tel.: +46-500-44-8547 ; fax: +46-500-44-8598 .*E-mail address*: bernard.schmidt@his.se .

Abstract

In today's manufacturing environment, safe human-robot collaboration is of paramount importance, to improve efficiency and flexibility. Targeting the safety issue, this paper presents an approach for human-robot collaboration in a shared workplace in close proximity, where real data driven 3D model of a robot and multiple depth images of the workplace are used for monitoring and decision-making to perform a task. The strategy for robot control depends on the current task and the information about the operator's presence and position. A case study of assembly is carried out in a robotic assembly cell with human collaboration. The results show that this approach can be applied in real-world applications such as human-robot collaborative assembly with human operators safeguarded at all time.

Keywords: Collision Avoidance; Human-Robot Collaboration

1. Introduction

In any human-robot collaborative environment where humans and robots coexist, safety protection of human operators in real time is of paramount importance. The challenge is not only collision detection in real time but collision avoidance at runtime via active closed-loop robot control.

During the past years, several approaches were reported for human-robot collaborations. Bussy [1] proposed a control scheme for humanoid robot to perform a transportation task jointly with a human partner. Takata and Hirano [2] proposed a planning algorithm that can allocate humans and robots in a hybrid assembly system, adaptively. Chen et al. [3] presented a simulation based multi objective optimisation process for allocating the assembly subtasks to both human and robot. Krüger et al. [4] summarised the advantages of human-robot collaboration in assembly lines. A hybrid assembly system exhibits both the efficiency of robots and the flexibility of humans. Nevertheless, it may induce extra stress to human operators if the assembly lines are improperly designed. Arai et al. [5] thus assessed operator stress from the perspective of distance and speed between a robot and an operator, aiming to guide the design of a productive hybrid assembly system.

Among safety monitoring and protection in human-robot collaborative manufacturing environment, two approaches were popularly used, i.e. vision-based approach such as 3D surveillance [6] via motion, colour and texture analysis, and inertial sensor-based approach [7] via a motion capture suit. From the practical point of view, the latter may not be feasible for real-world applications due to its dependence on a special suit with sensors and the limitation of motion capture of the suit wearer only, where the surrounding is unmonitored. This may lead to a safety leak, e.g. a mobile object may hit a stationary operator.

Efficient collision detection has been the focus for many years in vision-based approaches. Ebert et al. [8] proposed an emergency-stop approach to avoid a collision using an ad-hoc developed vision chip, whereas Gecks and Henrich [9] adopted a multi-camera system for detecting obstacles. Vogel et al. [10] presented a projector-camera based approach for dynamic safety zone boundary projection and violation detection. Tan and Arai [11] applied a triple stereovision system for tracking the upper-body movement of a sitting operator wearing a suit with colour markers. However, mobile operators that might appear in a monitored area may not

doi:10.1016/j.procir.2013.06.030

show consistent colour or texture. Moreover, changes in illumination may also affect the overall effectiveness of the collision-detection process. For this reason, range imaging with depth information is robust to the change in both colour and illumination, and allows straight representation of a view in 3D spaces. Schiavi et al. [12] used a ToF (time-of-flight) camera in implementation of a collision detection system. Fischer and Henrich [13] presented an approach using multiple 3D depth images for collision detection. For the range imaging, laser scanners provide high resolution but with relatively low processing speed, because each point or line of the scanned scene is sampled separately. Comparatively, ToF cameras allow acquiring depth images with high speed, but with low image resolution (up to 200×200) and with relatively high cost. Lately, Rybski et al. [14] fused data from stereo and range cameras to obtain a volumetric evidence grid for localisation of object and collision detection. Flacco et al. [15] presented an integrated framework for collision avoidance with use of single Kinect depth sensor and depth space approach without representing obstacles in the 3D space.

One of common choices from available commercial safety protection systems is SafetyEYE® [16]. It calculates 3D data about a surveilled space from three cameras embedded into sensing device and checks for intrusions into predefined safety zones. Entry into a safety zone may limit the movement speed or trigger an emergence stop of a robot in the zone. During active surveillance, the safety zones are static and cannot be changed.

For the purpose of close human-robot collaboration without sacrificing its productivity, there is a need to develop a cost-effective yet real-time safety solution suitable for dynamic manufacturing environment where human operators co-exist with robots.

Targeting the need, this research proposes a new approach for human safety protection. Its novelty includes: (1) timely collision detection between 3D models and depth images in augmented environment; and (2) active collision avoidance via path modification and robot control in real-time with zero robot programming.

The rest of the paper is organised as follows. Section 2 describes the collision detection; Section 3 provides the collision avoidance method; Section 4 depicts system implementation and test results; and finally, Section 5 concludes the paper and highlights our future work.

2. Collision detection

2.1. Depth images processing

The procedures of depth images acquisition and processing are illustrated in Fig. 1. Efficient processing is enabled by background removal with background images obtained during the calibration process. Objects corresponding to the moving robot are also removed from the depth images by the back projection of the robot model to images. After the background removal, only the foreign objects are left in the depth images, as shown in the second row of the right column in Fig. 1. The third row images reveal a mobile operator as the interested subject after applying a noise-removal filter and connected component algorithm.

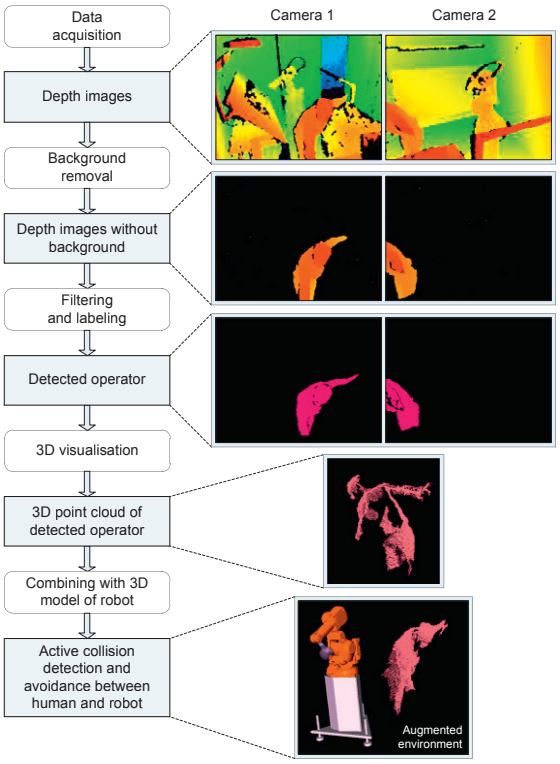

Fig. 1. Procedures of depth images processing.

The depth images of the detected operator from both cameras are converted to point clouds in the robot coordinate system, and merged into a single 3D point cloud after image registration. Finally, the single 3D point cloud of the operator is superimposed to the 3D model of the robot in augmented virtuality, where the minimum distance between the point cloud and the 3D robot model is calculated. The bottom image in Fig. 1 demonstrates the result of the depth images processing.

2.2. Minimum distance calculation

Although the size of the depth images is significantly reduced after background removal etc., the point cloud of the operator is still consisting of a large amount of data. To heuristically speed up the computation of collision detection, minimum bounding boxes are

applied to the 3D point cloud. In the current implementation, axis alignment bounding box is chosen for faster computation and easier representation by only two opposite corners. Fig. 2 depicts the point cloud with bounding boxes at different granularity. The actual level of granularity relates to the sensitivity of the collision detection, and is governed by a threshold parameter. To speed up the distance calculation, each of the subdivided boxes is treated as a minimal sphere bounding this sub-box. In this case, it only needs to calculate distance to the centre of each sub-box.

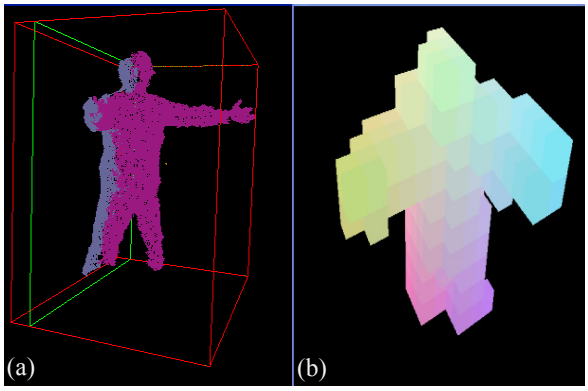

Fig. 2. (a) Point cloud in a minimum bounding box; (b) An array of subdivided boxes.

2.3. Sensitivity analysis

The depth cameras adopted in this research are Kinect sensors with spatial resolution 640×480, depth 11-bit, field of view 58×40 deg., and measurement range 0.8–3.5 m, as presented in Fig. 3. Since the Kinect sensors do not provide explicit distance values, a calibration is needed. This is carried out through measurements of a target surface from varying distances, where Eq. 1 is used for parameter optimisation to reduce errors in distance measurement.

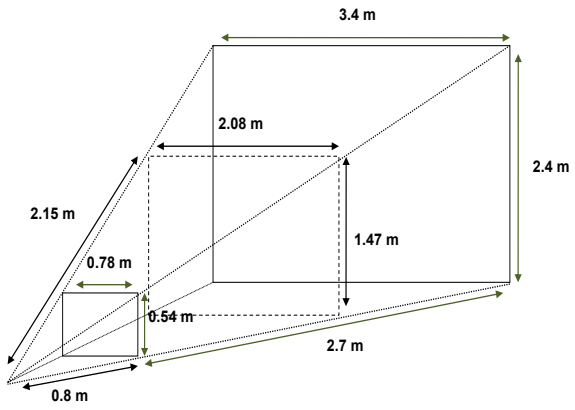

Fig 3. Kinect sensor's field of view.

$$d = k_3 \tan\left(\frac{n}{k_2} + k_1\right) - k_4 \quad (1)$$

where n is the raw 11-bit disparity from the Kinect sensor and k_1–k_4 are the calibration parameters whose optimised values are listed in Table 1.

Table 1. Parameters for Kinect sensor calibration

Parameter	Value		Unit
	Kinect 1	Kinect 2	
k_1	1.1873	1.18721	rad
k_2	2844.7	2844.1	1/rad
k_3	0.12423	0.1242	m
k_4	0.0045	0.01	m

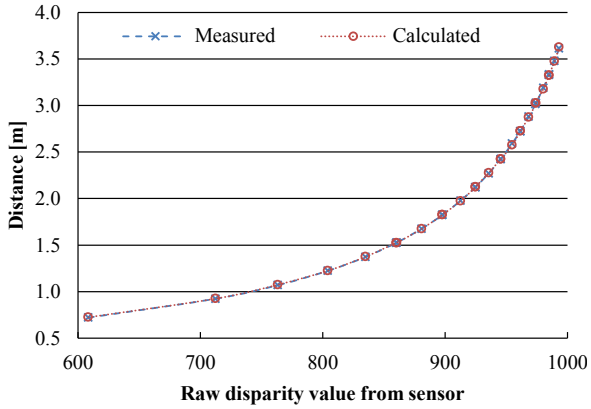

Fig. 4. Calibration results of distance measurement.

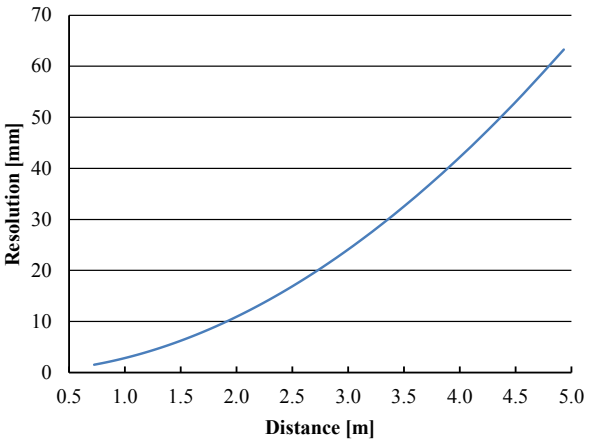

Fig. 5. Range resolutions of one Kinect sensor.

The calibration results of distance measurement and range resolutions of one of the Kinect sensors are given

in Fig. 4 and Fig. 5, respectively. When deciding a safety threshold value, both the workplace situation and the range resolutions as shown in Fig. 5 must be considered so as not to compromise the safety.

3. Collision avoidance

For the assembly operation, we can distinguish two behaviour scenarios of collision avoidance. The first is to stop the robot movement when the close proximity of an operator has been detected, and continue the robot movement after the operator walked away. This scenario is suitable for operations with limited degree of freedom, for example inserting. The second scenario is applicable to such operations as transportation where the path can be dynamically modified to avoid collision with human operators and other obstacles.

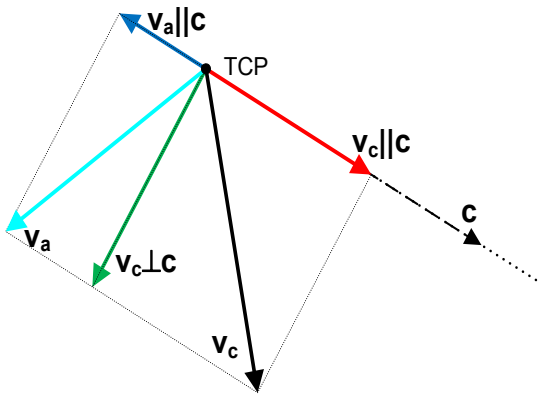

Fig. 6. Collision avoidance vectors.

When an obstacle is detected, a decision to modify the current robot path is taken based on the distance to the obstacle. The representation of vectors taken into consideration for path modification is shown in Fig. 6. Collision vector **c** is calculated, as vector between the TCP of the robot and the closest obstacle. The vector representing the direction of the robot movement $\mathbf{v_c}$ is decomposed into a parallel component $\mathbf{v_c}\|\mathbf{c}$ and a perpendicular component $\mathbf{v_c}\perp\mathbf{c}$ to the collision vector **c**. The parallel component is calculated in Eq. 2 as a dot product of the movement vector and collision versor and has the direction of the collision vector. Collision versor is a unit vector with direction of collision vector. Then the perpendicular component can be calculated using Eq. 3. The parallel component, as it is responsible for the movement towards the obstacle, is modified to avoid a collision. Modification is based on the distance from the obstacle and the direction of the movement and it gives as a result vector $\mathbf{v_a}\|\mathbf{c}$. Vector for modified movement is composed from $\mathbf{v_c}\perp\mathbf{c}$ and $\mathbf{v_a}\|\mathbf{c}$ as given in Eq. 4.

$$\mathrm{v_c} \parallel c = \left(\mathrm{v_c} \cdot \hat{c}\right) \cdot \hat{c}\,, \text{ where } \hat{c} = \frac{c}{\|c\|} \tag{2}$$

$$\mathrm{v_c} \perp c = \mathrm{v_c} - \mathrm{v_c} \parallel c \tag{3}$$

$$\mathrm{v_a} = \mathrm{v_a} \parallel c + \mathrm{v_c} \perp c \tag{4}$$

Example on how the parallel component of the movement vector is modified based on the distance to the obstacle is shown in Fig. 7. The line marked by ❶ is the desired movement in direction to the obstacle, and line ❷ is the desired movement in the opposite direction. Two threshold values d_{th1}, d_{th2} are used for modifying the parallel component of the movement vector. When the distance to the obstacle $\|\mathbf{c}\|$ is bigger than d_{th2}, the parallel component stays unchanged. When the distance is smaller than d_{th1}, the parallel component has the configured value with direction opposite to the obstacle. For the distance within the range of the two thresholds, the parallel component is changed linearly in the way to keep the dependence function continuous.

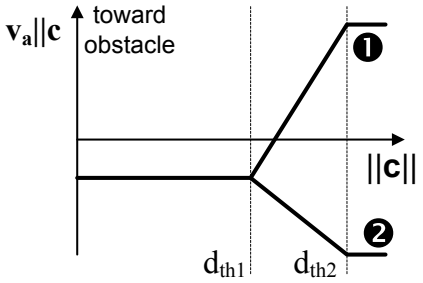

Fig. 7. Modification of the vector.

4. Robotic assembly testing

4.1. System configuration

The proposed active collision avoidance system is integrated with our earlier Wise-ShopFloor framework [17] as shown in Fig. 8. An ABB industrial robot IRB 140 is used to create a mini assembly cell for testing and validation. The application server of collision avoidance is deployed in a PC with Intel Core i7 CPU of 2.7 GHz, 4 GB RAM, and running a 64-bit Windows 7 operating system.

Two parallel tasks running in the robot controller for robot control and monitoring are expanded to handle the active collision avoidance. This third parallel task is added for independent communication with the collision avoidance application as shown in Fig. 9.

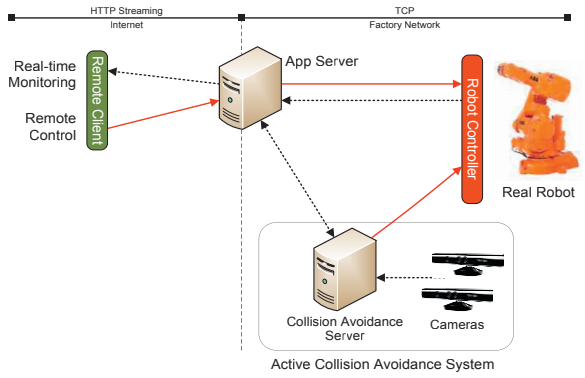

Fig. 8. System configuration.

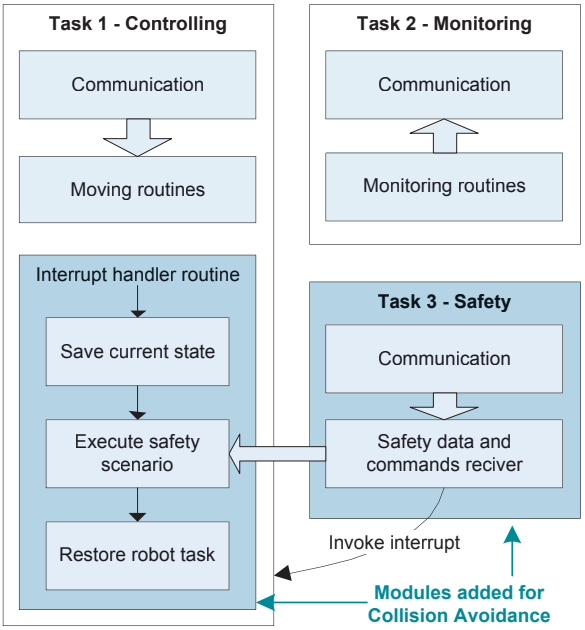

Fig. 9. Tasks structure of the robot controller.

A test case was performed in a robotic mini assembly cell as shown in Fig. 10, where a robot is assembling shafts and washers and inserting them in the magazine of finished products. A human operator is responsible for taking out the finished products from the magazine of the finished products as well as filling the magazines of components at the left-hand side. For the operation of picking and inserting, the collision avoidance is limited only to stop the movement of the robot arm. During the movement to/from the magazines, the active collision avoidance algorithm is applied.

Another exemplary scenario for assembly of the shafts and washers utilises the capability of the system to follow the operator. The robot has to grab a washer and deliver it to the human operator. The robot first grips a shaft and moves it to the human operator, who then inserts the washer on the shaft held by the robot. Afterwards, the robot takes the assembled product and puts it in the magazine of finished products. The delivery of the washer is realised by tracking and following the human operator's position. When the washer is gripped by the human operator, the robot releases the washer. This action can be triggered by a switch on the end-effector or by a voice command.

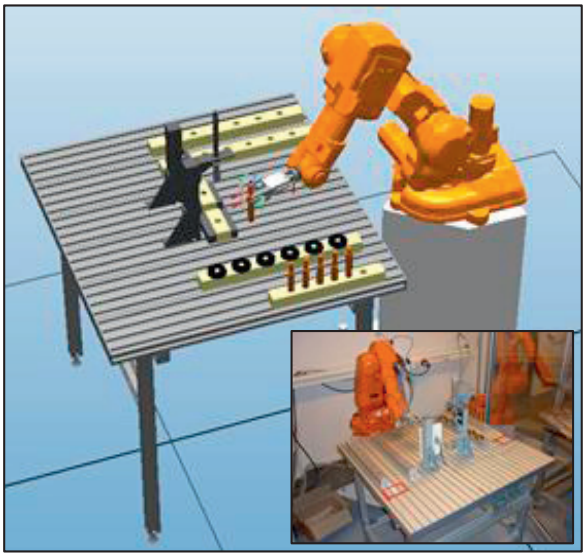

Fig. 10. A mini robotic assembly cell.

4.2. Results

A recorded example of the robot's TCP path during collision avoidance is shown in Fig. 11. The starting position of the robot is market by ⓪, following targets on the robot path are accordingly ①, ②, and back to ①. When there is no detected obstacle, robot moves linearly ❶ between specified targets. As soon as the presence of an obstacle is detected in proximity to the TCP, the current direction of movement is modified to avoid the collision on the way to the next target. Points of modified path are marked by circles ❷. Obstacle points taken into consideration during path modification are marked by crosses ❸; they are the closest points to the robot TCP. Lines ❹ represent the distances between the TCP and the obstacle during the movement.

The recorded results of the robot's TCP following an operator are shown in Fig. 12. The detected points of the operator's hand are marked by red crosses. The clusters of these points indicated by ①, ② and ③ correspond to the places where the operator held his hand for longer periods of time. The points of the robot TCP are marked by blue crosses, where ❶, ❷ and ❸ are the robot TCP's stopping points corresponding to the hand positions.

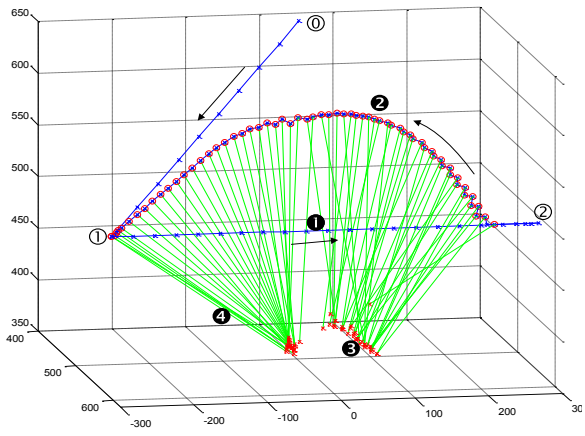

Fig.11. Recorded path for collision avoidance.

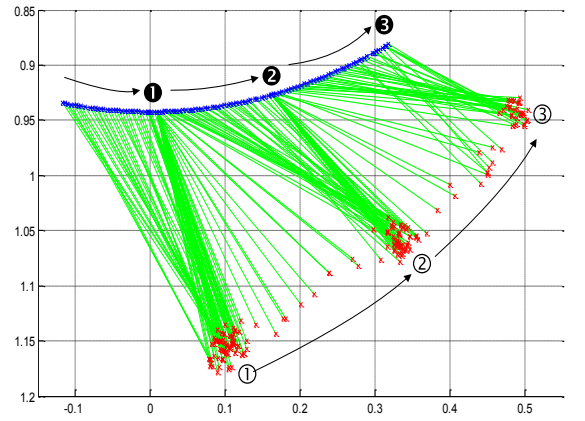

Fig.12. Recorded path for following.

5. Conclusions

This paper presents an integrated and cost-effective approach for real-time active collision avoidance in a human-robot collaborative work cell that enables all-time safety protection. This approach connects virtual 3D models to a set of motion and vision sensors for real-time monitoring and collision detection in augmented virtuality, aiming to improve the overall manufacturing performance. Rather than emergency stops that prevent human-robot coexistence, our approach links collision detection to active robot control through three collision-avoidance strategies: warning an operator, stopping a robot, or modifying the robot path to avoid a collision with the operator. The outcomes of the human-robot collaborative assembly are much improved flexibility, absolute human safety without a fence, and better overall productivity.

Our future work will focus more on developing and improving the collision avoidance strategies for more complicated collaborative manufacturing tasks.

References

[1] Bussy A., Kheddar A., Crosnier A., Keith F., 2012. Human-humanoid haptic joint object transportation case study, IEEE/RSJ International Conference on Intelligent Robots and Systems, p. 3633.

[2] Takata S., Hirano T., 2011. Human and Robot Allocation Method for Hybrid Assembly Systems. CIRP Annals – Manufacturing Technology 60(1), p. 9.

[3] Fei C., Sekiyama K:, Sasaki H., Jian H., Baiqing S., Fukuda T., 2011. Assembly strategy modeling and selection for human and robot coordinated cell assembly, IEEE/RSJ International Conference on Intelligent Robots and Systems, p. 4670.

[4] Krüger J., Lien T.K., Verl A., 2009. Cooperation of Human and Machines in Assembly Lines. CIRP Annals – Manufacturing Technology 58(2), p. 628.

[5] Arai T., Kato R., Fujita M., 2010. Assessment of Operator Stress Induced by Robot Collaboration in Assembly. CIRP Annals – Manufacturing Technology 59(1), p. 5.

[6] Krüger J., Nickolay B., Heyer P., 2005. Image Based 3D Surveillance for Flexible Man-Robot-Cooperation. Annals of the CIRP 54(1), p. 19.

[7] Corrales J.A., Candelas F.A., Torres F., 2011. Safe Human-Robot Interaction Based on Dynamic Sphere-Swept Line Bounding Volumes. Robotics and Computer-Integrated Manufacturing 27(1), p. 177.

[8] Ebert D., Komuro T., Namiki A., Ishikawa M., 2005. Safe Human-Robot-Coexistence: Emergency-Stop Using a High-Speed Vision-Chip. IEEE/RSJ International Conference on Intelligent Robots and Systems, p. 2923.

[9] Gecks T., Henrich D., 2005. Human-Robot Cooperation: Safe Pick-and-Place Operations. IEEE International Workshop on Robot and Human Interactive Communication, p. 549.

[10] Vogel C., Poggendorf M., Walter C., Elkmann N., 2011. Towards safe physical human-robot collaboration: A projection-based safety system, IEEE/RSJ International Conference on Intelligent Robots and Systems, p. 3355.

[11] Tan J.T.C., Arai T., 2011. Triple Stereo Vision System for Safety Monitoring of Human-Robot Collaboration in Cellular Manufacturing. IEEE/CIRP International Symposium on Assembly and Manufacturing, p. 1.

[12] Schiavi R., Bicchi A., Flacco F., 2009. Integration of Active and Passive Compliance Control for Safe Human-Robot Coexistence. IEEE International Conference on Robotics and Automation, p. 259.

[13] Fischer M., Henrich D., 2009. 3D Collision Detection for Industrial Robots and Unknown Obstacles Using Multiple Depth Images. Advances in Robotics Research (Kröger T, Wahl FM, Eds) 111.

[14] Rybski P., Anderson-Sprecher P., Huber D., Niessl C., Simmons R., 2012. Sensor fusion for human safety in industrial workcells, IEEE/RSJ International Conference on Intelligent Robots and Systems, p. 3612.

[15] Flacco F., Kröger T., De Luca A., Khatib O., 2012. A Depth Space Approach to Human-Robot Collision Avoidance. IEEE International Conference on Robotics and Automation, p 338

[16] Pilz GmbH & Co. KG (2006) http://www.safetyeye.com/

[17] Wang L., Givehchi M., Adamson G., Holm M., 2011. A Sensor-Driven 3D Model-Based Approach to Remote Real-Time Monitoring. CIRP Annals – Manufacturing Technology 60(1), p. 493.